

# The Farnesoid X Receptor Regulates Adipocyte Differentiation and Function by Promoting Peroxisome Proliferator-activated Receptor- $\gamma$ and Interfering with the Wnt/ $\beta$ -Catenin Pathways<sup>\*[5]</sup>

Received for publication, July 21, 2010, and in revised form, August 27, 2010. Published, JBC Papers in Press, September 17, 2010, DOI 10.1074/jbc.M110.166231

Mouaadh Abdelkarim<sup>‡§||</sup>, Sandrine Caron<sup>‡§||</sup>, Christian Duhem<sup>‡§||</sup>, Janne Prawitt<sup>‡§||</sup>, Julie Dumont<sup>‡§||</sup>, Anthony Lucas<sup>‡§||</sup>, Emmanuel Bouchaert<sup>‡§||</sup>, Olivier Briand<sup>‡§||</sup>, John Brozek<sup>\*\*</sup>, Folkert Kuipers<sup>‡‡</sup>, Catherine Fievet<sup>‡§||</sup>, Bertrand Cariou<sup>‡§||1</sup>, and Bart Staels<sup>‡§||2</sup>

From the <sup>‡</sup>Université Lille Nord de France, F-59000 Lille, France, the <sup>§</sup>INSERM, UMR1011, F-59019 Lille, France, the <sup>||</sup>Université Droit Santé Lille 2, F-59000 Lille, France, the <sup>||</sup>Institut Pasteur de Lille, F-59019 Lille, France, <sup>\*\*</sup>Genfit, 59120 Loos, France, and the <sup>‡‡</sup>Center for Liver, Digestive and Metabolic Diseases, Laboratory of Pediatrics, University Medical Center Groningen, 9713 GZ Groningen, The Netherlands

The bile acid receptor farnesoid X receptor (FXR) is expressed in adipose tissue, but its function remains poorly defined. Peroxisome proliferator-activated receptor- $\gamma$  (PPAR $\gamma$ ) is a master regulator of adipocyte differentiation and function. The aim of this study was to analyze the role of FXR in adipocyte function and to assess whether it modulates PPAR $\gamma$  action. Therefore, we tested the responsiveness of FXR-deficient mice (FXR<sup>-/-</sup>) and cells to the PPAR $\gamma$  activator rosiglitazone. Our results show that genetically obese FXR<sup>-/-</sup>/ob/ob mice displayed a resistance to rosiglitazone treatment. *In vitro*, rosiglitazone treatment did not induce normal adipocyte differentiation and lipid droplet formation in FXR<sup>-/-</sup> mouse embryonic fibroblasts (MEFs) and preadipocytes. Moreover, FXR<sup>-/-</sup> MEFs displayed both an increased lipolysis and a decreased *de novo* lipogenesis, resulting in reduced intracellular triglyceride content, even upon PPAR $\gamma$  activation. Retroviral-mediated FXR re-expression in FXR<sup>-/-</sup> MEFs restored the induction of adipogenic marker genes during rosiglitazone-forced adipocyte differentiation. The expression of Wnt/ $\beta$ -catenin pathway and target genes was increased in FXR<sup>-/-</sup> adipose tissue and MEFs. Moreover, the expression of several endogenous inhibitors of this pathway was decreased early during the adipocyte differentiation of FXR<sup>-/-</sup> MEFs. These findings demonstrate that FXR regulates adipocyte differentiation and function by regulating two counteracting pathways of adipocyte differentiation, the PPAR $\gamma$  and Wnt/ $\beta$ -catenin pathways.

The nuclear receptor farnesoid X receptor (FXR)<sup>3</sup> is a transcription factor that belongs to the nuclear receptor superfamily that is endogenously activated by bile acids (1). FXR was initially found to regulate bile acid metabolism and to protect the liver from the deleterious effect of excessive bile acid accumulation (2–4). The phenotype of FXR-deficient (FXR<sup>-/-</sup>) mice further established a role for FXR in lipid metabolism (5). Recently, FXR was shown to be implicated in the control of hepatic glucose metabolism and peripheral insulin sensitivity (6–9). FXR modulates the fasting-refeeding transition in mice (8), and genetic murine models of diabetes display an increased FXR expression (10). Although FXR deficiency was associated with peripheral insulin resistance (6, 7), activation of FXR by bile acids (6) or specific synthetic agonists (7, 9) conversely improves glucose homeostasis in rodent models of diabetes. Finally, FXR appears to be involved in the regulation of adaptive thermogenesis in response to fasting or cold exposure (11).

The primary role of adipose tissue is to store energy in form of triglycerides (TG) in the adipocytes, which can be liberated as fatty acids upon energy requirement. Adipose tissue is also an endocrine organ secreting hormones involved in metabolic homeostasis (12). Preadipocyte differentiation into mature adipocytes is a finely tuned process that is regulated by a complex network of transcription factors. In this cascade, the peroxisome proliferator-activated receptor- $\gamma$  (PPAR $\gamma$ ) (13) and CAAT/enhancer-binding protein (C/EBP)  $\alpha$  (14) act as key regulators. Early regulators of preadipocyte differentiation are other members of the CAAT/enhancer-binding protein family, C/EBP $\beta$  and C/EBP $\delta$  (15), which induce the expression of PPAR $\gamma$  and C/EBP $\alpha$  (16). Among the extracellular signaling pathways that regulate adipogenesis is the Wnt pathway (17). The non-canonical and canonical Wnt signaling pathways, being respectively  $\beta$ -catenin-independent and -dependent, are negative regulators of adipogenesis (17). In the absence of Wnt

\* This work was supported by European Union Grant HEPADIP 018734, COST Action Grant BM0602, and Agence Nationale de la Recherche Grant A05056GS. This work was also supported by a grant from the Fondation pour la Recherche Médicale (to M. A.).

[5] The on-line version of this article (available at <http://www.jbc.org>) contains supplemental Tables 1 and 2.

<sup>1</sup> Present address: INSERM U915, IRTUN, l'Institut du Thorax, 8 Quai Moncousu BP70721, 44007 Nantes Cedex 1, France.

<sup>2</sup> To whom correspondence should be addressed: UMR1011 INSERM, Institut Pasteur de Lille, 1 rue du Professeur Calmette, BP245, 59019 Lille, France. Tel.: 33-3-20-87-73-88; Fax: 33-3-20-87-73-60; E-mail: Bart.Staels@pasteur-lille.fr.

<sup>3</sup> The abbreviations used are: FXR, farnesoid X receptor; PPAR $\gamma$ , peroxisome proliferator-activated receptor- $\gamma$ ; MEF, mouse embryonic fibroblast; TG, triglyceride(s); C/EBP, CAAT/enhancer-binding protein; sFRP, secreted Frizzled-related protein; RSG, rosiglitazone; ADRP, adipose differentiation-related protein.

## FXR Controls Adipose PPAR $\gamma$ Responsiveness

proteins,  $\beta$ -catenin is localized in the cytoplasm in a protein complex containing Axin and adenomatous polyposis coli (APC) proteins, which facilitate  $\beta$ -catenin phosphorylation and its subsequent proteasomal degradation (18). The binding of Wnt proteins to their receptors Frizzled (FZD) and low density lipoprotein receptor-related protein-5 or -6 (LRP5/6) leads to  $\beta$ -catenin protein stabilization. Hypophosphorylated  $\beta$ -catenin protein translocates into the nucleus and activates its target genes (19). The activation of Wnt/ $\beta$ -catenin signaling leads to the repression of adipogenesis by blocking the induction of PPAR $\gamma$  and C/EBP $\alpha$  expression (20). On the other hand, PPAR $\gamma$  activation leads to proteasomal-dependent  $\beta$ -catenin degradation by stimulating the activity of GSK3 $\beta$ , a  $\beta$ -catenin kinase, and by interacting with phospho- $\beta$ -catenin itself (20–22). A finely regulated balance between  $\beta$ -catenin activity and PPAR $\gamma$  expression is thus required for proper adipocyte differentiation (23).

We (7) and others (24) have shown that FXR is expressed in adipocyte, where it modulates adipocyte differentiation (7, 24). FXR expression was found to be decreased in adipose tissue of mouse models of dietary and genetic obesity (7). FXR expression is induced during adipocyte differentiation in 3T3-L1 cells and mouse embryonic fibroblasts (MEFs) (7, 24). MEFs isolated from FXR $^{-/-}$  mice (FXR $^{-/-}$  MEFs) display an impaired adipocyte differentiation with a delay in the expression of adipogenic genes and a decreased lipid droplet size (7). Additionally, FXR activation in 3T3-L1 cells during adipocyte differentiation by specific synthetic agonists increases mRNA expression of adipogenic genes, as well as insulin signaling and insulin-stimulated glucose uptake (7, 24).

In the present study, we provide *in vivo* evidence that FXR was necessary for a full response to PPAR $\gamma$  activation. We show that obese FXR $^{-/-}$ /*ob/ob* mice displayed an altered response to PPAR $\gamma$  activation by rosiglitazone. Retroviral re-expression of FXR in FXR $^{-/-}$  MEFs restored the adipogenic gene expression program in response to rosiglitazone. The delay in adipogenic differentiation in FXR $^{-/-}$  MEFs was associated with a sustained activation of Wnt/ $\beta$ -catenin signaling. All these results provide evidence for a crucial role of FXR in adipogenesis by promoting the PPAR $\gamma$  pathway and interfering with Wnt/ $\beta$ -catenin signaling.

## EXPERIMENTAL PROCEDURES

**Animals**—Female and male *ob/ob* mice (B6.V-Lepob/J) from Charles River (Saint Aubin les Elseuf, France) were crossed with FXR $^{+/+}$  and FXR $^{-/-}$  C57BL6/J mice to obtain FXR $^{+/+}$ /*ob/ob* and FXR $^{-/-}$ /*ob/ob* mice. 12-week-old FXR $^{-/-}$ /*ob/ob* female mice and their wild type littermates ( $n = 7$ /group) were housed on a 12-h light/12-h dark cycle with free access to water and were treated with the PPAR $\gamma$  agonist rosiglitazone (Avandia<sup>®</sup>, GlaxoSmithKline) (10 mg/kg of body weight) mixed with control diet (UAR A03, Villemoisson/Orge, France) for 21 days.

**Isolation and Culture of MEFs**—MEFs were derived from 13.5-day-old FXR $^{+/+}$  and FXR $^{-/-}$  embryos (C57BL6/N) (7). MEFs were plated in 6-well plates at 300,000 cells/well. Adipocyte differentiation was initiated 2 days after confluence with AmnioMAX-C100 medium (Invitrogen), 7.5% AmnioMAX-C100 supplement, 7.5% fetal bovine serum (FBS), 0.5 mM

3-isobutyl-1-methylxanthine, 1  $\mu$ M dexamethasone, 5  $\mu$ g/ml insulin. From days 3–8, cells were incubated with AmnioMAX-C100 medium with 5  $\mu$ g/ml insulin and 1  $\mu$ M rosiglitazone. At days 0, 4, and 8, cells were used for lipid metabolism studies (lipolysis, *de novo* lipogenesis, and triglyceride content), lysed and homogenized for RNA isolation, or fixed in 4% paraformaldehyde and stained with Oil Red O. All experiments were performed in triplicate.

**Preadipocyte Isolation and Culture**—Preadipocytes were isolated from inguinal fat pads of 20-week-old FXR $^{-/-}$ /*ob/ob* and their FXR $^{+/+}$ /*ob/ob* littermates. Adipose tissue was isolated, dissociated mechanically, and digested in Krebs buffer solution (118 mM NaCl, 5 mM KCl, 1.25 mM CaCl<sub>2</sub>, 1.2 mM KH<sub>2</sub>PO<sub>4</sub>, 1.2 mM MgSO<sub>4</sub>, 20 mM NaHCO<sub>3</sub>, 2 mM sodium pyruvate, 10 mM HEPES, 3% BSA, pH 7.4) containing 1.5 mg/ml collagenase A (Roche Diagnostics GmbH, Mannheim, Germany) for 1.5 h in a shaking water bath at 37 °C. After digestion, the mature adipocytes were separated from the stroma-vascular cells by centrifugation. The stroma-vascular pellet containing the preadipocytes was treated with erythrocyte lysis solution (154 mmol/liter NH<sub>4</sub>Cl, 10 mmol/liter KHCO<sub>3</sub>, 0.1 mmol/liter EDTA) for 5 min at room temperature and centrifuged. The preadipocyte-containing pellet was cultured in PromoCell<sup>®</sup> preadipocyte growth medium (PromoCell GmbH, Heidelberg, Germany) at 37 °C in a humidified 95% air and 5% CO<sub>2</sub> incubator. Cultures were grown to confluence (days (–2)). Two days after confluence (day 0), the medium was changed to preadipocyte differentiation medium supplemented with 8  $\mu$ g/ml D-biotin-4, 0.5  $\mu$ g/ml bovine insulin, 400 ng/ml dexamethasone, 44  $\mu$ g/ml 3-isobutyl-1-methylxanthine, 9 ng/ml L-thyroxine. From days 3–8, the medium was changed to adipocyte nutrition medium and was supplemented with rosiglitazone (1  $\mu$ M). At days 0, 4, and 8, cells were lysed and homogenized for RNA isolation or fixed in 4% paraformaldehyde and stained with Oil Red O.

**Measurement of Triglyceride Content**—Cellular lipids were extracted with hexane/isopropyl alcohol (3:2 v/v). Lipids were then dried with nitrogen gas, redissolved in isopropyl alcohol, and quantified using the TG PAP 1000 kit (BioMérieux, Marcy l'Etoile, France).

**Lipolysis Assay**—Lipolysis experiments were performed at days 4 and 8 of MEF differentiation. Cells were washed with PBS and incubated with 300  $\mu$ l of incubation solution (adipolysis assay kit, OB100, Millipore) with 2% BSA or containing 10  $\mu$ M isoproterenol for 3 h. Glycerol was measured in the culture supernatant with free glycerol assay reagent (adipolysis assay kit, OB100, Millipore). Glycerol concentrations were normalized to total cellular protein content. All experiments were performed in triplicate.

**De Novo Lipogenesis Assay**—*De novo* lipogenesis was evaluated by measuring incorporation of radiolabeled acetate precursor into total cellular lipids. Cells were washed and incubated with compounds for 48 h in culture medium without FBS and with 3 mg/ml BSA. Cells were then washed and incubated in Krebs-Ringer buffer for 90 min in the presence of 1  $\mu$ Ci of [<sup>14</sup>C]acetate (Amersham Biosciences, Saclay, France). MEFs were washed, and total cellular lipids were extracted twice with hexane/isopropyl alcohol. The pooled organic fractions were transferred to scintillation vials, dried under nitrogen, and

assessed for radioactivity by liquid scintillation counting. [ $^{14}$ C]Acetate incorporation was normalized to total cellular protein content.

**Real Time Quantitative Reverse Transcription-PCR**—Total RNA was isolated from white adipose tissue using the acid guanidinium thiocyanate/phenol/chloroform method and from MEFs and differentiated preadipocytes using the TRIzol reagent (Invitrogen) and subsequently reverse-transcribed using Moloney murine leukemia virus (Applied Biosystems, Paris, France). cDNAs were quantified by quantitative PCR on a Mx4000 apparatus (Stratagene) using specific primers (supplemental Table 2). mRNA levels were subsequently normalized to those of cyclophilin.  $\Delta$ Ct was calculated as the difference between the Ct of the gene of interest and that of cyclophilin.

**Plasmid and Retrovirus Infection**—The retrovirus was constructed using the FXR $\alpha$ 3 mouse cDNA. The sequences of the primers used were: 5'-atcgcggatccatggtgatgagtttcagg-3' and 5'-ctctagaccctacagctcactcagctgcgcata-3' (the initiation (atg) and stop (tag) codons are underlined). The FXR coding sequence was cloned into the mammalian expression vector pBabe-Puro (Invitrogen) in BamHI and Sall sites. Human embryonic kidney 293T modified packaging cells (Ecotropic Phoenix) were cultured in Dulbecco's modified Eagle's medium (DMEM) containing 10% FBS and transiently transfected with a pBabe-puro-FXR chimera or a pBabe-puro vector alone as negative control. 48 h after transfection, the viral supernatant was harvested and used to infect the MEFs. Selection of MEFs that had incorporated the retrovirus was done by adding puromycin to the medium for 1 week. FXR expression was measured by quantitative PCR.

**Treatment with sFRP1 Recombinant Protein**—Recombinant human secreted Frizzled-related protein (sFRP) 1 was purchased from R&D Systems (Minneapolis, MN). FXR $^{-/-}$  MEFs were differentiated in the presence or absence of recombinant sFRP1 (75 nmol/liter) added at day 0.

**Western Blot**—Total cellular MEF protein was extracted using a radioimmune precipitation assay buffer (50 mM Tris-HCl, 150 mM NaCl, 1.0% (v/v) Nonidet P-40, 0.5% (w/v) sodium deoxycholate, 1.0 mM EDTA, 0.1% (w/v) SDS, and 0.01% (w/v) sodium azide, pH:7.4). Protein concentration was determined by the Bradford method (Bio-Rad protein assay). Protein samples were denatured by heating to 90 °C in SDS-reducing buffer and resolved by electrophoresis on 10% SDS-polyacrylamide gels. After protein transfer, nitrocellulose membranes were incubated with a mouse monoclonal anti- $\beta$ -catenin antibody (catalog number 610153, BD Transduction Laboratories) for 3 h and HRP-conjugated secondary antibody (Dako A/S, Glostrup, Denmark) for 1 h. Proteins were then visualized by chemiluminescence using an ECL detection kit (Amersham Biosciences, Orsay, France).

**Adipocyte Size Determination**—Inguinal adipose tissue was fixed in 4% neutral buffered paraformaldehyde, embedded in paraffin, cut into 7- $\mu$ m sections, and stained with hematoxylin. Cell size was determined using the ImageJ software (National Institutes of Health, Bethesda, MD, rsb.info.nih.gov/ij).

**Microarray Analysis**—Total RNA was prepared from epididymal adipose tissue of FXR $^{+/+}$  and FXR $^{-/-}$  mice, and the subsequent steps were performed as described elsewhere (25). Affymetrix raw data were normalized using the robust multiar-

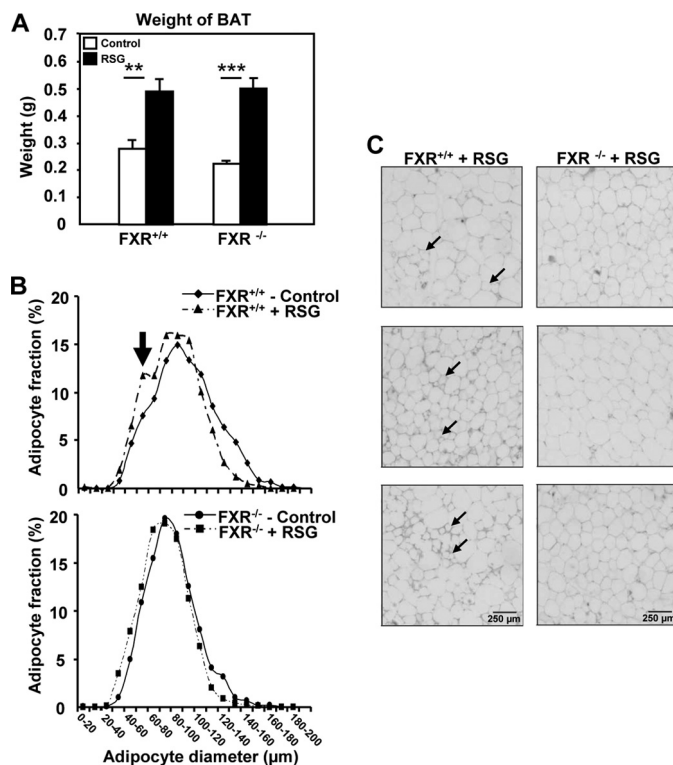


**FIGURE 1. Obese FXR $^{-/-}$ /ob/ob mice are resistant to the effects of PPAR $\gamma$  activation on adipocyte recruitment.** A, increase of brown adipose tissue (BAT) mass in FXR $^{-/-}$  and FXR $^{+/+}$ /ob/ob mice after rosiglitazone (RSG) treatment. B, adipocyte size distribution in adipose tissue of FXR $^{-/-}$  and FXR $^{+/+}$ /ob/ob mice treated or not with RSG. 200 adipocytes were studied per section. Adipocyte size was measured using ImageJ. C, morphology of white adipocytes of FXR $^{-/-}$  and FXR $^{+/+}$ /ob/ob mice ( $n = 3$ /group) treated with RSG (10 mg/kg). Small adipocytes recruited after RSG treatment are indicated by the arrow. \*\*,  $p < 0.01$ ; \*\*\*,  $p < 0.001$ .

ray average (RMA) algorithm to obtain expression values in log $_2$  (26). Log $_2$ -transformed expression values were fitted to a linear model according to Limma package methods (Bioconductor). A model was established to identify probesets significantly differentially expressed between FXR $^{+/+}$  and FXR $^{-/-}$  mice. False discovery rate correction was applied to take into account multiple testing hypotheses. Selection of relevant probe sets was based on a mean log $_2$  expression value greater than 6.12 in a least one of the two compared conditions, a  $p$  value  $< 10^{-5}$ , and an absolute -fold change value of 1.5. Function of all clustering of regulated genes was performed by Ingenuity Pathway Analysis (Ingenuity).

**Statistical Analysis**—Statistical significance was analyzed using the unpaired Student's  $t$  test. All values are reported as means  $\pm$  S.D. Values with  $p < 0.05$  were considered significant.

## RESULTS

**FXR Deficiency Results in a Partial Resistance to PPAR $\gamma$  Activation in Adipose Tissue in Vivo**—To explore whether the FXR and PPAR $\gamma$  pathways interact *in vivo*, genetically obese (ob/ob) FXR $^{-/-}$  and FXR $^{+/+}$  mice were treated with rosiglitazone (10 mg/kg of body weight) for 21 days. As a positive control of *in vivo* PPAR $\gamma$  activation (27), mice from both genotypes displayed a comparable increase of brown adipose tissue mass (Fig. 1A), a tissue that does not express FXR (11, 28). As expected (7), adipose tissue of FXR $^{-/-}$  mice contained a larger proportion of

## FXR Controls Adipose PPAR $\gamma$ Responsiveness

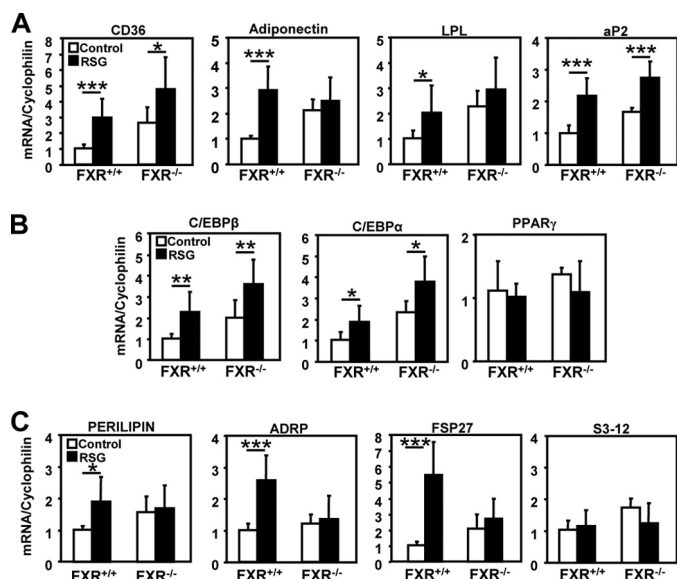


**FIGURE 2. FXR deficiency alters the expression profile of white adipose tissue genes following rosiglitazone treatment.** A–C, mRNA expression of PPAR $\gamma$  target genes (A), adipogenic transcription factor genes (B), and lipid droplet genes (C) in white adipose tissue of FXR<sup>-/-</sup> and FXR<sup>+/+</sup> *ob/ob* mice after rosiglitazone treatment. mRNA levels were measured by quantitative PCR. Values are normalized to the expression of cyclophilin and are expressed relative to control FXR<sup>+/+</sup> mice. LPL, lipoprotein lipase. \*,  $p < 0.05$ ; \*\*,  $p < 0.01$ ; \*\*\*,  $p < 0.001$ .

small adipocytes (average diameter  $78 \pm 21 \mu\text{m}$ ) than FXR<sup>+/+</sup> adipose tissue (average diameter  $90 \pm 26 \mu\text{m}$ ) (Fig. 1B and supplemental Table 1). Interestingly, although PPAR $\gamma$  activation by rosiglitazone led to the appearance of a subpopulation of smaller adipocytes in white adipose tissue of FXR<sup>+/+</sup> mice, likely due to the induction of preadipocyte recruitment (29), this response was not observed in FXR<sup>-/-</sup> mice (Fig. 1, B and C, and supplemental Table 1). Moreover, the induction of some PPAR $\gamma$  target genes such as adiponectin and lipoprotein lipase (LPL) by rosiglitazone was abolished in adipose tissue from FXR<sup>-/-</sup> when compared with FXR<sup>+/+</sup> mice (Fig. 2A). Although the induction of other PPAR $\gamma$  target genes (*cd36* and *aP2*) was also reduced in FXR<sup>-/-</sup> mice, the expression of adipogenic genes, such as C/EBP $\alpha$  and C/EBP $\beta$ , was induced to the same level in both genotypes, and PPAR $\gamma$  expression itself was not modified (Fig. 2B). Most interestingly, the induction of genes involved in lipid droplet formation, such as perilipin, adipose differentiation-related protein (ADRP), and *fsp27*, by rosiglitazone was totally abolished in FXR<sup>-/-</sup> when compared with FXR<sup>+/+</sup> mice, whereas *s3-12* expression was not affected (Fig. 2C). These data demonstrate that FXR is necessary to ensure the full response to PPAR $\gamma$  activation in adipose tissue.

**FXR Deficiency Results in an Impaired Responsiveness to PPAR $\gamma$  Activation in MEFs in Vitro**—To study whether FXR modulates adipocyte PPAR $\gamma$  responsiveness in a cell-autonomous manner, MEFs were isolated from FXR<sup>+/+</sup> and FXR<sup>-/-</sup> embryos and differentiated into adipocytes with or without rosiglitazone, and the expression of adipocyte differentiation markers was measured. As expected (7), FXR<sup>-/-</sup> MEFs were resistant to adipocyte differentiation with a lower expression of C/EBP $\alpha$ , PPAR $\gamma$ , and *aP2* at day 4 of differentiation in the absence of rosiglitazone (Fig. 3). Upon PPAR $\gamma$  activation, the

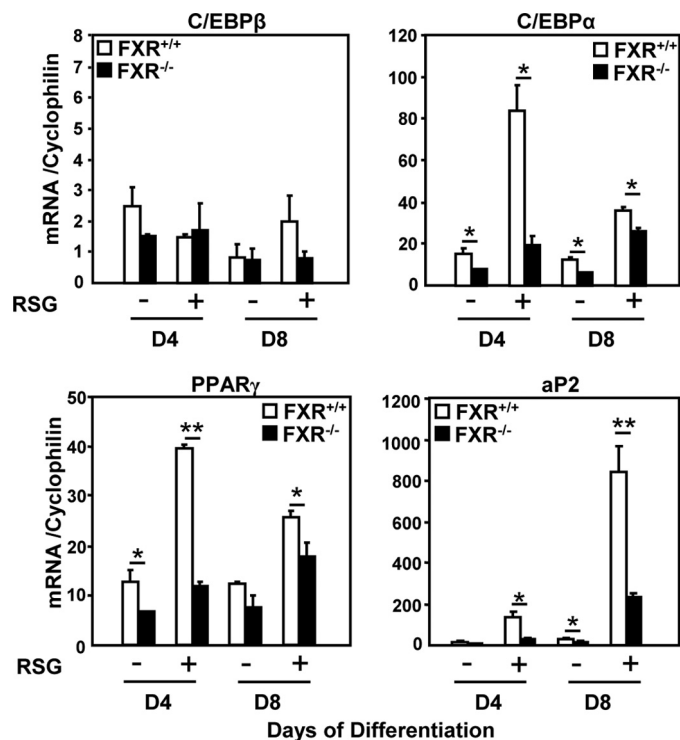


**FIGURE 3. FXR<sup>-/-</sup> MEFs are resistant to PPAR $\gamma$  activation.** mRNA levels of adipogenic genes of 4- and 8-day-differentiated FXR<sup>-/-</sup> and FXR<sup>+/+</sup> MEFs in the presence or absence of  $1 \mu\text{M}$  RSG were measured by quantitative PCR. Values are normalized to the expression of cyclophilin and are expressed relative to those at day 0, which are arbitrarily set to 1. These results are representative of three experiments. \*,  $p < 0.05$ ; \*\*,  $p < 0.01$ .

induction of C/EBP $\alpha$ , PPAR $\gamma$ , and *aP2* following rosiglitazone treatment was drastically reduced at day 4, and to a lesser extent at day 8, in FXR<sup>-/-</sup> when compared with FXR<sup>+/+</sup> MEFs (Fig. 3). These results show that FXR<sup>-/-</sup> MEFs are resistant to PPAR $\gamma$  activation, which is unable to induce the complete adipogenic differentiation program in these cells.

**FXR<sup>-/-</sup> MEFs Exhibit a Reduced Lipid Storage Capacity upon PPAR $\gamma$  Activation**—The functional consequences of the resistance to PPAR $\gamma$  activation was studied by comparing the phenotype of FXR<sup>-/-</sup> and FXR<sup>+/+</sup> MEFs differentiated in the presence of rosiglitazone. The increase in TG content at day 8 of differentiation was significantly lower in FXR<sup>-/-</sup> MEFs when compared with FXR<sup>+/+</sup> MEFs (Fig. 4A). This reduction in TG content can be the consequence of either an increase in TG degradation (lipolysis) and/or a decrease in TG synthesis (lipogenesis). Therefore, basal and  $\beta$ -adrenergically (isoproterenol)-induced lipolysis was assessed by measuring glycerol release into the cell culture medium. Rosiglitazone-treated FXR<sup>-/-</sup> MEFs displayed an enhanced lipolysis when compared with FXR<sup>+/+</sup> MEFs under both basal conditions and after  $\beta$ -adrenergic stimulation (Fig. 4A), which was statistically significant at day 4 of differentiation. Analysis of [<sup>14</sup>C]acetate incorporation demonstrated a significant decrease of fatty acid synthesis (*de novo* lipogenesis) in rosiglitazone-treated FXR<sup>-/-</sup> when compared with FXR<sup>+/+</sup> MEFs at days 4 and 8 of differentiation (Fig. 4A). Moreover, PPAR $\gamma$ -activated FXR<sup>-/-</sup> MEFs also exhibited an abnormal morphology with lipid droplets of smaller size (Fig. 4B). Accordingly, rosiglitazone-treated FXR<sup>-/-</sup> MEFs showed decreased expression of several lipid

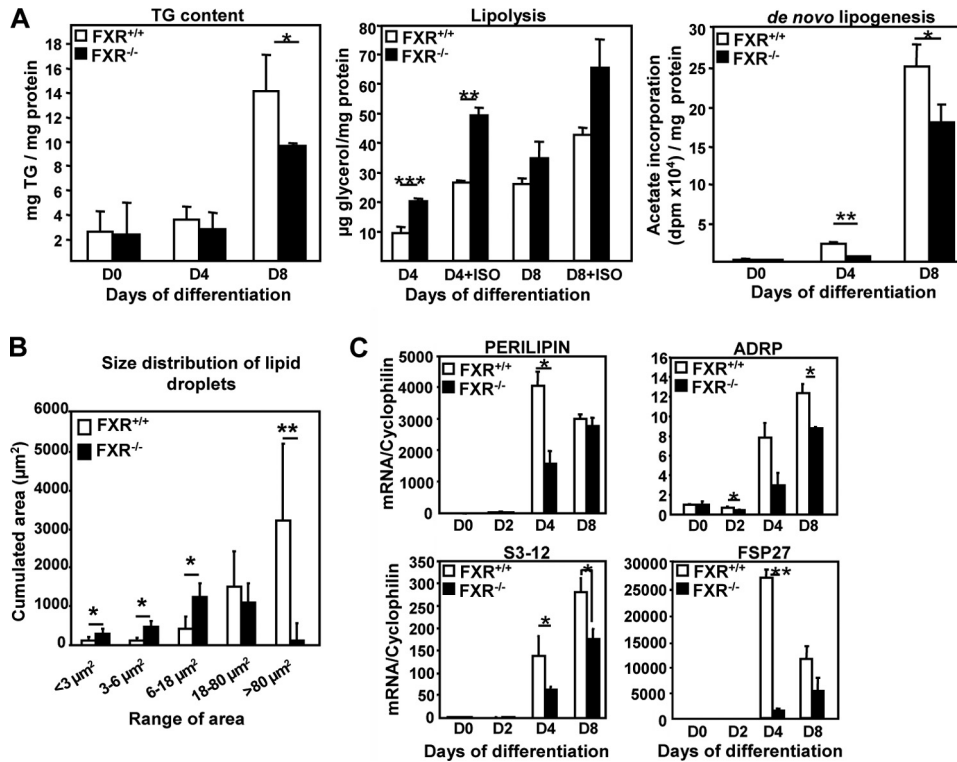


**FIGURE 4. FXR deficiency alters triglyceride storage, lipolysis, de novo lipogenesis, and the expression of lipid droplet genes in MEFs during differentiation to adipocytes.** A, TG content in FXR<sup>-/-</sup> and FXR<sup>+/+</sup> MEFs at days 0, 4, and 8 of differentiation treated with 1  $\mu$ M rosiglitazone; lipolysis was measured in FXR<sup>-/-</sup> and FXR<sup>+/+</sup> MEFs at days 0, 4, and 8 as glycerol release under basal and stimulated (isoproterenol: ISO) conditions. De novo lipogenesis in FXR<sup>-/-</sup> and FXR<sup>+/+</sup> MEFs was measured at days 0, 4, and 8 of differentiation. The results are representative of three experiments and are presented as means  $\pm$  S.D. B, quantification of the lipid droplet size of 8-day-differentiated FXR<sup>-/-</sup> and FXR<sup>+/+</sup> MEFs. C, mRNA expression of genes coding for lipid droplet proteins in FXR<sup>-/-</sup> and FXR<sup>+/+</sup> MEFs during differentiation measured by quantitative PCR. Values are normalized to the expression of cyclophilin and are expressed relative to those at day 0, which are arbitrarily set to 1. The results are representative of three experiments. \*,  $p < 0.05$ ; \*\*,  $p < 0.01$ ; \*\*\*,  $p < 0.001$ .

droplet genes at day 4, such as perilipin, ADRP, and TIP47 (PAT) protein family (30), and *fsp27* (31), a member of the recently identified cell death-inducing DFF45-like effector (CIDE) protein family (Fig. 4C). Although perilipin gene expression did not differ between the two genotypes at day 8, ADRP and *s3-12* gene expression was still significantly reduced (Fig. 4C). These results indicate that FXR plays a critical role in developing a full lipid storage capacity during adipocyte differentiation by controlling the PPAR $\gamma$ -mediated formation of lipid droplets.

**FXR<sup>-/-</sup> Preadipocytes Display Impaired Adipocyte Differentiation upon PPAR $\gamma$  Activation**—To determine whether FXR deficiency also impairs primary adipocyte differentiation upon PPAR $\gamma$  activation, preadipocytes were isolated from the stromal fraction of inguinal adipose tissue of FXR<sup>-/-</sup>/*ob/ob* and FXR<sup>+/+</sup>/*ob/ob* littermates and differentiated into adipocytes in the presence of rosiglitazone. C/EBP $\beta$  and C/EBP $\alpha$  mRNA levels were clearly lower at days 4 and 8 of differentiation in FXR<sup>-/-</sup> when compared with FXR<sup>+/+</sup> cells, whereas the reduction of PPAR $\gamma$  and *aP2* expression reached significance only at day 4 (Fig. 5A). As in differentiated MEFs, 8-day-differentiated rosiglitazone-treated FXR<sup>-/-</sup> adipocytes exhibited an abnormal morphology with smaller lipid droplets when compared with FXR<sup>+/+</sup> cells (Fig. 5B). This phenotype was associated with a transiently reduced expression of the perilipin and

*fsp27* genes at day 4, whereas ADRP and *S3-12* gene expression was not affected (Fig. 5C). Surprisingly, FSP27 mRNA levels were found to be increased at day 8 in FXR<sup>-/-</sup> adipocytes. Altogether, these results show that FXR<sup>-/-</sup> preadipocytes display altered adipocyte differentiation even when PPAR $\gamma$  is activated.

**Reintroduction of FXR in FXR<sup>-/-</sup> MEFs Restores the Expression of Adipogenic and Lipid Droplet Genes and Increases the Number of Differentiated Adipocyte Clusters**—To determine whether the altered adipocyte differentiation observed in rosiglitazone-treated FXR<sup>-/-</sup> MEFs was strictly FXR-dependent, FXR was exogenously (re-)expressed in FXR<sup>-/-</sup> and FXR<sup>+/+</sup> MEFs using a retrovirus encoding FXR $\alpha$ 3, which, together with FXR $\alpha$ 4, is expressed in MEF cells (data not shown). Infected cells were subsequently subjected to adipogenic differentiation in the presence of rosiglitazone. Retroviral infection led to a pronounced mRNA expression of FXR $\alpha$ 3 in FXR<sup>-/-</sup> MEFs during adipocyte differentiation, with a 3-fold higher expression at day 8 when compared with FXR<sup>+/+</sup> MEFs infected with

empty retrovirus (data not shown). Importantly, reintroduction of FXR resulted in an increased number of differentiated adipocyte clusters (Fig. 6A) and a restoration of PPAR $\gamma$  and *aP2* expression at day 8, whereas neither the expression of C/EBP $\beta$  nor the expression of C/EBP $\alpha$  was affected in FXR<sup>-/-</sup> MEFs (Fig. 6B). Moreover, the expression of all lipid droplet genes was significantly increased at day 8 (Fig. 6C). Thus, re-expression of FXR in FXR<sup>-/-</sup> MEFs restores the capacity of MEFs to differentiate into adipocytes upon rosiglitazone treatment.

**FXR Deficiency Results in a Dysregulation of the Wnt/ $\beta$ -Catenin Pathway in Adipose Tissue and Adipocytes**—To unravel the mechanisms underlying the impaired adipocyte differentiation linked to FXR deficiency, a microarray analysis was performed in white adipose tissue from FXR<sup>-/-</sup> versus FXR<sup>+/+</sup> mice to identify pathways with altered expression (data not shown). One of those identified is the Wnt/ $\beta$ -catenin signaling pathway known to inhibit adipocyte differentiation at least in part by inhibiting PPAR $\gamma$  activity (19). Indeed, mRNA levels of  $\beta$ -catenin were increased in adipose tissue of FXR<sup>-/-</sup> versus FXR<sup>+/+</sup> obese mice (Fig. 7A). In accordance with an increased Wnt/ $\beta$ -catenin signaling, mRNA levels of *lrp5* and *Axin2* (18), both target genes and components of the Wnt/ $\beta$ -catenin pathway, and the target genes *cyclin D1* and *c-myc* (32, 33), were higher in adipose tissue of FXR<sup>-/-</sup> when compared with FXR<sup>+/+</sup> mice (Fig. 7A).

## FXR Controls Adipose PPAR $\gamma$ Responsiveness

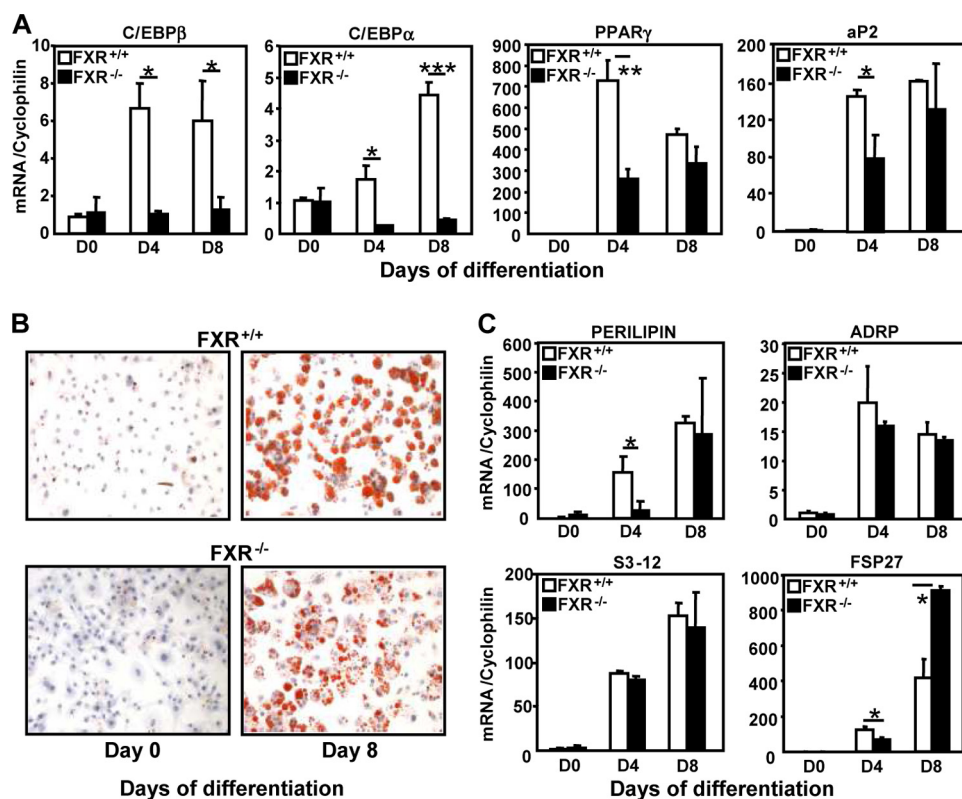


**FIGURE 5. FXR deficiency impairs PPAR $\gamma$ -induced differentiation and lipid droplet formation of primary preadipocytes.** A and C, expression of adipogenic marker (A) and lipid droplet protein (C) genes in FXR<sup>-/-</sup> when compared with FXR<sup>+/+</sup> preadipocytes treated with 1  $\mu$ M rosiglitazone. Preadipocytes were isolated from white adipose tissue of obese FXR<sup>-/-</sup>/ob/ob and FXR<sup>+/+</sup>/ob/ob mice. mRNA levels were measured by quantitative PCR. Values ( $\pm$  S.D.) are normalized to the expression of cyclophilin and are expressed relative to those at day 0, which are arbitrarily set to 1. B, smaller size of lipid droplets in FXR<sup>-/-</sup> when compared with FXR<sup>+/+</sup> preadipocytes. Representative Oil Red O staining of FXR<sup>-/-</sup> and FXR<sup>+/+</sup> preadipocytes at days 0 and 8 of differentiation is shown ( $\times 20$  magnification). \*,  $p < 0.05$ ; \*\*,  $p < 0.01$ ; \*\*\*,  $p < 0.001$ .

The expression of regulators and components of the Wnt/ $\beta$ -catenin pathway was also analyzed during the differentiation of FXR<sup>+/+</sup> and FXR<sup>-/-</sup> MEFs into adipocytes. Interestingly, the expression of sFRP1 and sFRP5, negative regulators of the Wnt pathway, was lower in FXR<sup>-/-</sup> MEFs during early adipocyte differentiation, at days 2 and 1, respectively (Fig. 7B). In parallel, Western blot analysis showed that  $\beta$ -catenin protein expression was higher in FXR<sup>-/-</sup> MEFs with a peak at day 4 when compared with FXR<sup>+/+</sup> MEFs (Fig. 7C). In accordance with an increased Wnt/ $\beta$ -catenin signaling, the expression of *lrp5*, *Axin2*, *cyclin D1*, and *c-myc*, four target genes of this pathway, was increased in FXR<sup>-/-</sup> when compared with FXR<sup>+/+</sup> MEFs (Fig. 7D). Moreover, restoration of FXR expression in FXR<sup>-/-</sup> MEFs using the FXR $\alpha$ 3-encoding retrovirus resulted in a decrease of  $\beta$ -catenin protein expression (Fig. 7E) along with the improvement of adipocyte differentiation (Fig. 6B). Moreover, mRNA expression of the Wnt/ $\beta$ -catenin pathway genes *c-myc*, *Axin2*, and *lrp5* decreased upon FXR reintroduction in FXR<sup>-/-</sup> MEFs (Fig. 7E). To further assess whether the anti-adipogenic effect of FXR deficiency is mediated by the activation of the Wnt/ $\beta$ -catenin signaling pathway, we investigated whether the secreted Wnt antagonist sFRP1 could reverse this effect. The elevated  $\beta$ -catenin protein expression in FXR<sup>-/-</sup> when compared with FXR<sup>+/+</sup> MEFs was reduced upon incubation with recombinant sFRP1 protein (Fig. 8A). Concomitantly,

sFRP1 treatment of FXR<sup>-/-</sup> MEFs increased the expression of adipogenic markers, such as PPAR $\gamma$  and *aP2* (Fig. 8B). These results demonstrate that the Wnt/ $\beta$ -catenin pathway, which inhibits adipocyte differentiation and PPAR $\gamma$  function, is activated in FXR-deficient adipocytes *in vivo* and *in vitro* and that restoration of FXR expression inhibits the Wnt signaling pathway.

## DISCUSSION

The results of this study identify a role for the nuclear receptor FXR as a modulator of the PPAR $\gamma$  and Wnt signaling pathways in adipocyte differentiation. FXR<sup>-/-</sup> mice displayed an impaired response to PPAR $\gamma$  activation, and FXR<sup>-/-</sup> MEFs were resistant to the induction of adipogenic differentiation by PPAR $\gamma$  activation. Our results show that lipid storage is impaired in FXR<sup>-/-</sup> MEFs even after PPAR $\gamma$  activation due to decreased *de novo* lipogenesis and increased lipolysis. Microarray analysis of adipose tissue from FXR<sup>+/+</sup> and FXR<sup>-/-</sup> mice allowed us to identify that FXR deficiency alters mRNA expression of genes implicated in the Wnt/ $\beta$ -catenin signaling pathway. FXR<sup>-/-</sup>

adipose tissue and FXR<sup>-/-</sup> MEFs exhibited an overactivation of the Wnt/ $\beta$ -catenin signaling pathway, an inhibitor of adipocyte differentiation and PPAR $\gamma$  function. These results demonstrate that FXR is critical for full adipocyte differentiation by promoting PPAR $\gamma$  activation and interfering with the Wnt/ $\beta$ -catenin signaling pathways.

Our study shows that FXR deficiency led to impaired adipocyte differentiation of MEFs, as well as preadipocytes isolated from the stromal fraction of FXR<sup>-/-</sup> adipose tissue, with a clear alteration of lipid droplet gene expression after differentiation in the presence of rosiglitazone. This alteration of mRNA expression in FXR<sup>-/-</sup> cells was already detectable at days 2 and 4, whereas the functional consequences reflected in lipid droplet morphology were observed later at day 8 of differentiation. This alteration of adipocyte differentiation induced by rosiglitazone was strictly FXR-dependent because FXR reintroduction improved differentiation of FXR<sup>-/-</sup> MEFs with an increased expression of adipogenic markers, such as PPAR $\gamma$  and *aP2*, and an increased number of differentiated cell clusters. Intriguingly, *C/EBP $\alpha$*  and *C/EBP $\beta$*  mRNA expression was not restored. We have currently no explanation for the lack of response of these two genes.

Rosiglitazone-treated FXR<sup>-/-</sup> MEFs displayed an alteration of triglyceride storage that was correlated with a combination of a decrease of *de novo* lipogenesis and an increase of lipolysis.

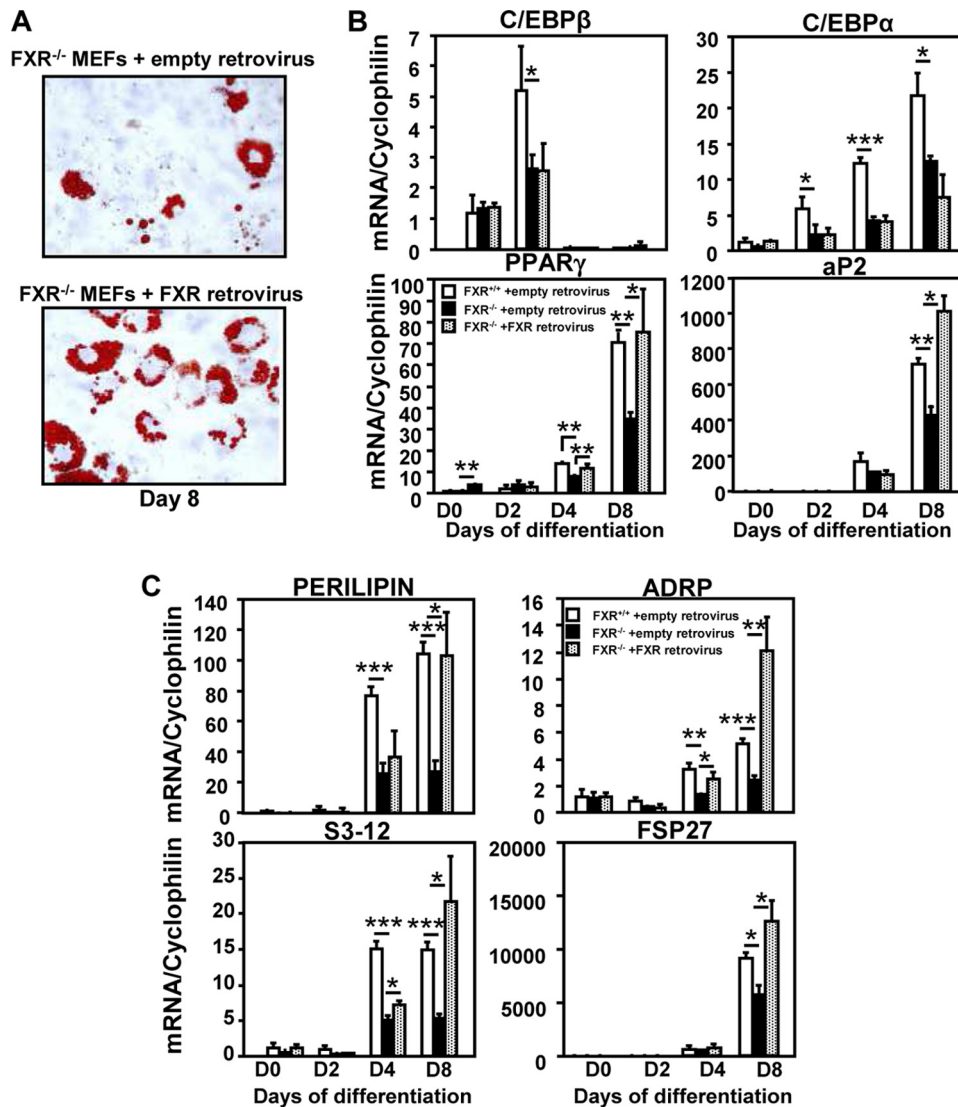


**FIGURE 6. Re-expression of FXR reverses the impaired adipocyte differentiation of rosiglitazone-treated FXR<sup>-/-</sup> MEFs.** FXR<sup>-/-</sup> MEFs were infected with a retrovirus coding for FXR $\alpha$ 3 or the empty vector, subjected to adipogenic differentiation, and treated with 1  $\mu$ M rosiglitazone. *A*, increased number of differentiated cell clusters after FXR retroviral infection of rosiglitazone-treated FXR<sup>-/-</sup> MEFs. Representative Oil Red O staining of FXR<sup>-/-</sup> and FXR<sup>+/+</sup> MEFs at day 8 of differentiation is shown ( $\times 20$  magnification). *B* and *C*, mRNA levels of adipogenic markers (*B*) and lipid droplet protein (*C*) genes in empty retrovirus- and FXR retrovirus-infected rosiglitazone-treated FXR<sup>-/-</sup> MEFs measured by quantitative PCR. Empty retrovirus-transfected FXR<sup>+/+</sup> MEFs were used as reference. Values are normalized to cyclophilin mRNA and are expressed relative to those at day 0, which are arbitrarily set to 1. The results are representative of three experiments. \*,  $p < 0.05$ ; \*\*,  $p < 0.01$ ; \*\*\*,  $p < 0.001$ .

In parallel, the expression of lipogenic genes was decreased in FXR<sup>-/-</sup> MEFs (data not shown). This result is in agreement with those obtained in the 3T3-L1 cell line showing an increase of lipogenic gene expression after treatment with FXR agonists (24).

FXR<sup>-/-</sup> MEFs exhibited an increase of both basal and  $\beta$ -adrenergically induced lipolysis. However, the extent of  $\beta$ -adrenergically mediated induction was similar between FXR<sup>-/-</sup> and FXR<sup>+/+</sup> MEFs, suggesting that downstream pathways are not influenced by FXR. However, the expression of lipid droplet genes such as perilipin, ADRP, *s3-12*, and *fsp27*, which play a role in lipid droplet formation and lipolysis, is altered even after PPAR $\gamma$  activation. Because FXR<sup>-/-</sup> MEFs and preadipocytes present a decreased lipid droplet size, it would be interesting to

determine the localization of the adipose triacylglycerol lipase (ATGL) and hormone-sensitive lipase (HSL) proteins before and after  $\beta$ -adrenergic stimulation. Indeed, a recent study proposes that these two enzymes are preferentially associated with small lipid droplets (34) and thus could contribute to the increase of lipolysis in FXR<sup>-/-</sup> adipocytes.

Microarray analysis of white adipose tissue of FXR<sup>+/+</sup> and FXR<sup>-/-</sup> mice showed that FXR deficiency is associated with impaired expression of regulators and components of the Wnt/ $\beta$ -catenin signaling pathway (35). Interestingly, the expression of sFRP5, an inhibitor of the Wnt/ $\beta$ -catenin signaling pathway, was down-regulated *in vivo* (data not shown) and *in vitro* in FXR<sup>-/-</sup> MEFs. Conversely,  $\beta$ -catenin, a gene implicated in inhibition of adipocyte differentiation and adipose tissue formation (35–37), was up-regulated in adipose tissue of FXR<sup>-/-</sup> mice. This observation is consistent with studies showing that there is an increase of  $\beta$ -catenin in the intestine of FXR<sup>-/-</sup> mice (38).

sFRP5 mRNA levels correlate with adiposity (39). Thus, the observed decrease of sFRP5 mRNA expression is in agreement with the description of lower adipose tissue mass in FXR<sup>-/-</sup> mice (7). Moreover, the expression of sFRP1, which, when overexpressed, induces spontaneous adipocyte differentiation (40), was decreased in FXR<sup>-/-</sup> MEFs. mRNA levels of sFRP1 and sFRP5 were decreased

respectively at days 2 and 1 of MEFs differentiation, which correlates with the increased  $\beta$ -catenin protein levels especially at day 4 of FXR<sup>-/-</sup> MEF differentiation. Moreover, incubation of FXR<sup>-/-</sup> MEFs with sFRP1 decreased  $\beta$ -catenin protein and increased expression of adipogenic genes. These results show that FXR acts at an early stage of the adipogenic program, at least in part by controlling the expression of negative regulators of Wnt/ $\beta$ -catenin signaling pathway.

Several lines of evidence indicate that the Wnt/ $\beta$ -catenin signaling pathway is increased in FXR<sup>-/-</sup> adipose tissue and MEF cells. The expression of the receptor, LRP5, the regulator of  $\beta$ -catenin stability and phosphorylation, Axin2, and the target genes of the Wnt/ $\beta$ -catenin signaling pathway, cyclin D1 and *c-myc*, were up-regulated in the absence of FXR. Cyclin D1 and

## FXR Controls Adipose PPAR $\gamma$ Responsiveness

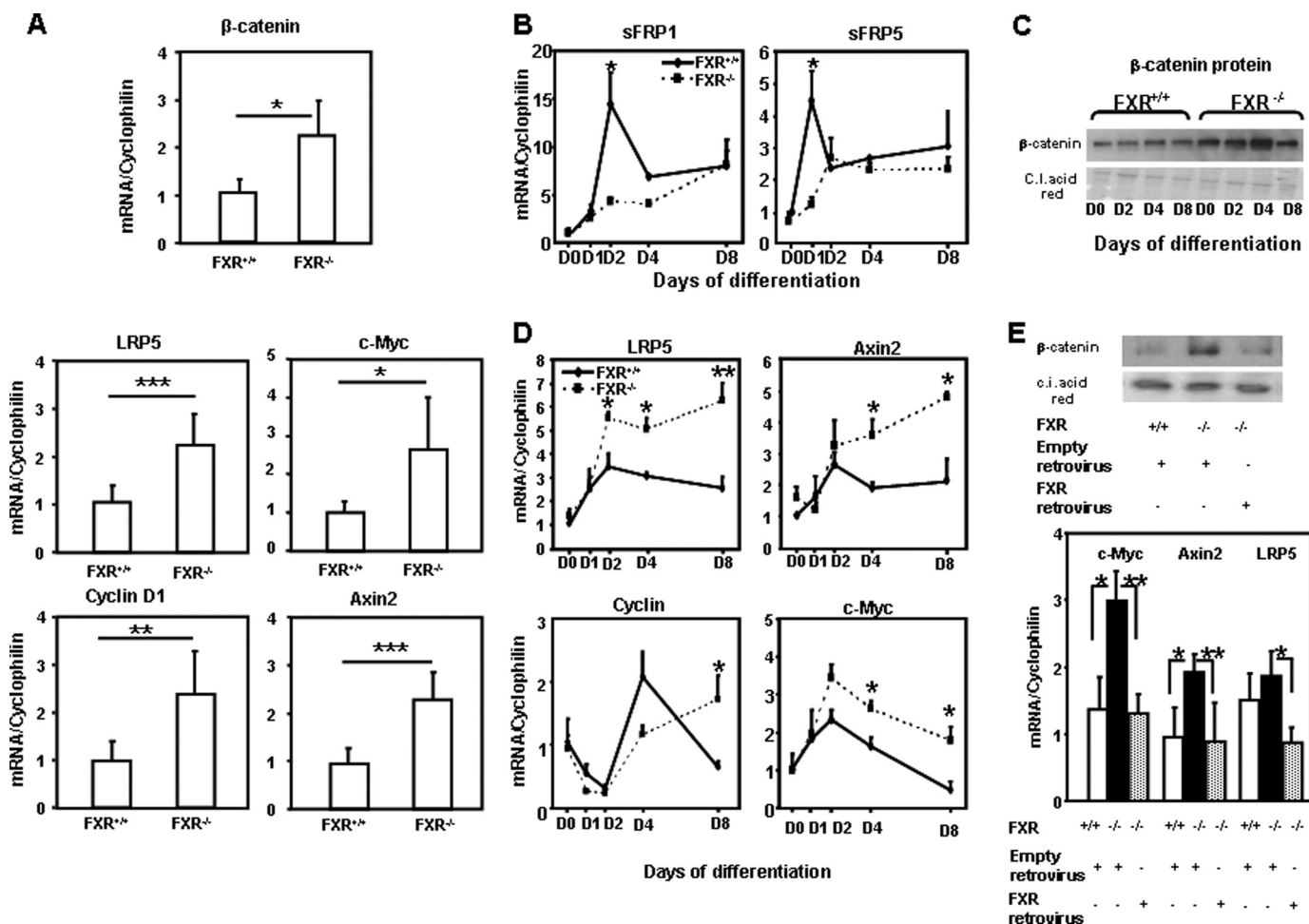


**FIGURE 7. Up-regulation of the Wnt/ $\beta$ -catenin signaling pathway in adipose tissue of  $FXR^{-/-}/ob/ob$  mice and  $FXR^{-/-}$  MEFs.** *A*, mRNA expression of  $\beta$ -catenin, LRP5, c-Myc, Axin2, and cyclin D1 in inguinal adipose tissue of  $FXR^{-/-}$  and  $FXR^{+/+}/ob/ob$  mice. mRNA levels were measured by quantitative PCR. Values are normalized to the expression of cyclophilin and are expressed relative to  $FXR^{+/+}$  mice, which are arbitrarily set to 1. The results are presented as means  $\pm$  S.D. *B*, mRNA expression of sFRP1 and sFRP5 during differentiation of  $FXR^{-/-}$  and  $FXR^{+/+}$  MEFs treated with 1  $\mu$ M rosiglitazone. *C*,  $\beta$ -catenin protein levels during  $FXR^{-/-}$  and  $FXR^{+/+}$  MEF differentiation. *D*, mRNA levels of Wnt/ $\beta$ -catenin target genes during differentiation of  $FXR^{-/-}$  and  $FXR^{+/+}$  MEFs. *E*, *top*,  $\beta$ -catenin protein levels. *Bottom*, mRNA levels of c-Myc, Axin2, and LRP5 in  $FXR^{+/+}$  and  $FXR^{-/-}$  MEFs transfected for 2 days with empty or FXR retrovirus as indicated. mRNA levels were measured by quantitative PCR. Values are normalized to those at day 0, which are arbitrarily set to 1. The results are representative of two experiments. \*,  $p < 0.05$ ; \*\*,  $p < 0.01$ ; \*\*\*,  $p < 0.001$ . C.I. acid red, Ponceau S.

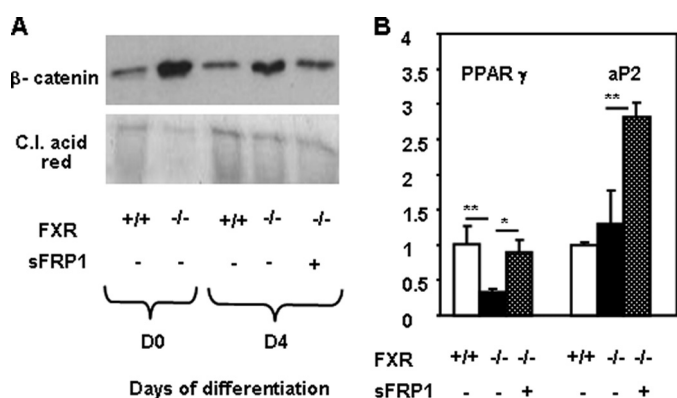


**FIGURE 8. sFRP1 reduces  $\beta$ -catenin protein (A) and increases PPAR $\gamma$  and aP2 gene expression in  $FXR^{-/-}$  MEFs (B).**  $FXR^{-/-}$  MEFs were differentiated in the presence or absence of recombinant sFRP1 (75 nmol/liter). *A*,  $\beta$ -catenin protein levels. *B*, mRNA levels of adipogenic genes measured by quantitative PCR. Values are normalized to the expression of cyclophilin and are expressed relative to those in  $FXR^{+/+}$  MEFs, which are arbitrarily set to 1. \*,  $p < 0.05$ ; \*\*,  $p < 0.01$ . C.I. acid red, Ponceau S.

c-Myc both inhibit adipocyte differentiation by decreasing PPAR $\gamma$  activity through histone deacetylase recruitment on the promoter of its target genes (32) and by suppressing C/EBP $\alpha$  and *p21* gene expression (41). These results suggest that FXR interferes with the activation of the Wnt/ $\beta$ -catenin signaling pathway to promote adipocyte differentiation. This interference could be mediated by a decrease of  $\beta$ -catenin protein stability via a feedback regulation affecting the expression and protein level of Axin2 or LRP5 or via the induction of GSK3 $\beta$ , the kinase that phosphorylates the  $\beta$ -catenin protein.

Another argument for the modulation of the Wnt/ $\beta$ -catenin signaling pathway is the observation that FXR deficiency results in an impaired responsiveness to PPAR $\gamma$  activation *in vitro* and *in vivo*. First, FXR deficiency altered PPAR $\gamma$  expression in MEFs, and FXR reintroduction in  $FXR^{-/-}$  MEFs increased mRNA expression of PPAR $\gamma$ . Moreover,  $FXR^{-/-}$  MEFs displayed a resistance to the induction of adipocyte differentiation

by rosiglitazone treatment. In the same line, FXR<sup>-/-</sup>/ob/ob mice exhibited an impaired responsiveness to PPAR $\gamma$  activation reflected by altered expression of several PPAR $\gamma$  target genes, including lipid droplet genes. These results further corroborate the existence of a cross-talk between FXR and PPAR $\gamma$  activities, as has been proposed in hepatocytes where FXR increases PPAR $\gamma$  expression, thereby regulating the antifibrotic activity of FXR in rodent liver (42).

In summary, FXR is necessary for a proper response to PPAR $\gamma$  activation, suggesting a cross-talk between FXR and PPAR $\gamma$ . Moreover, FXR contributes to the induction of adipocyte differentiation by interfering with the Wnt/ $\beta$ -catenin signaling pathway. These results identify a critical role for FXR in adipose tissue to ensure the accurate and complete course of adipocyte differentiation.

## REFERENCES

- Lefebvre, P., Cariou, B., Lien, F., Kuipers, F., and Staels, B. (2009) *Physiol. Rev.* **89**, 147–191
- Makishima, M., Okamoto, A. Y., Repa, J. J., Tu, H., Learned, R. M., Luk, A., Hull, M. V., Lustig, K. D., Mangelsdorf, D. J., and Shan, B. (1999) *Science* **284**, 1362–1365
- Wang, H., Chen, J., Hollister, K., Sowers, L. C., and Forman, B. M. (1999) *Mol. Cell* **3**, 543–553
- Parks, D. J., Blanchard, S. G., Bledsoe, R. K., Chandra, G., Consler, T. G., Kliewer, S. A., Stimmel, J. B., Willson, T. M., Zavacki, A. M., Moore, D. D., and Lehmann, J. M. (1999) *Science* **284**, 1365–1368
- Sinal, C. J., Tohkin, M., Miyata, M., Ward, J. M., Lambert, G., and Gonzalez, F. J. (2000) *Cell* **102**, 731–744
- Ma, K., Saha, P. K., Chan, L., and Moore, D. D. (2006) *J. Clin. Invest.* **116**, 1102–1109
- Cariou, B., van Harmelen, K., Duran-Sandoval, D., van Dijk, T. H., Grefhorst, A., Abdelkarim, M., Caron, S., Torpier, G., Fruchart, J. C., Gonzalez, F. J., Kuipers, F., and Staels, B. (2006) *J. Biol. Chem.* **281**, 11039–11049
- Duran-Sandoval, D., Cariou, B., Percevault, F., Hennuyer, N., Grefhorst, A., van Dijk, T. H., Gonzalez, F. J., Fruchart, J. C., Kuipers, F., and Staels, B. (2005) *J. Biol. Chem.* **280**, 29971–29979
- Zhang, Y., Lee, F. Y., Barrera, G., Lee, H., Vales, C., Gonzalez, F. J., Willson, T. M., and Edwards, P. A. (2006) *Proc. Natl. Acad. Sci. U.S.A.* **103**, 1006–1011
- Duran-Sandoval, D., Mautino, G., Martin, G., Percevault, F., Barbier, O., Fruchart, J. C., Kuipers, F., and Staels, B. (2004) *Diabetes* **53**, 890–898
- Cariou, B., Bouchaert, E., Abdelkarim, M., Dumont, J., Caron, S., Fruchart, J. C., Burcelin, R., Kuipers, F., and Staels, B. (2007) *FEBS Lett.* **581**, 5191–5198
- Halberg, N., Wernstedt-Asterholm, I., and Scherer, P. E. (2008) *Endocrinol. Metab. Clin. North Am.* **37**, 753–768
- Tontonoz, P., Hu, E., and Spiegelman, B. M. (1994) *Cell* **79**, 1147–1156
- Lin, F. T., and Lane, M. D. (1994) *Proc. Natl. Acad. Sci. U.S.A.* **91**, 8757–8761
- Wu, Z., Bucher, N. L., and Farmer, S. R. (1996) *Mol. Cell. Biol.* **16**, 4128–4136
- Lefterova, M. I., and Lazar, M. A. (2009) *Trends Endocrinol. Metab.* **20**, 107–114
- Christodoulides, C., Lagathu, C., Sethi, J. K., and Vidal-Puig, A. (2009) *Trends Endocrinol. Metab.* **20**, 16–24
- Logan, C. Y., and Nusse, R. (2004) *Annu. Rev. Cell Dev. Biol.* **20**, 781–810
- Angers, S., and Moon, R. T. (2009) *Nat. Rev. Mol. Cell Biol.* **10**, 468–477
- Liu, J., and Farmer, S. R. (2004) *J. Biol. Chem.* **279**, 45020–45027
- Sharma, C., Pradeep, A., Wong, L., Rana, A., and Rana, B. (2004) *J. Biol. Chem.* **279**, 35583–35594
- Farmer, S. R. (2005) *Int. J. Obes. (Lond.)* **29**, Suppl. 1, S13–S16
- Moldes, M., Zuo, Y., Morrison, R. F., Silva, D., Park, B. H., Liu, J., and Farmer, S. R. (2003) *Biochem. J.* **376**, 607–613
- Rizzo, G., Disante, M., Mencarelli, A., Renga, B., Gioiello, A., Pellicciari, R., and Fiorucci, S. (2006) *Mol. Pharmacol.* **70**, 1164–1173
- Slonim, D. K., Koide, K., Johnson, K. L., Tantravahi, U., Cowan, J. M., Jarrah, Z., and Bianchi, D. W. (2009) *Proc. Natl. Acad. Sci. U.S.A.* **106**, 9425–9429
- Irizarry, R. A., Bolstad, B. M., Collin, F., Cope, L. M., Hobbs, B., and Speed, T. P. (2003) *Nucleic Acids Res.* **31**, e15
- Lazarenko, O. P., Rzonca, S. O., Hogue, W. R., Swain, F. L., Suva, L. J., and Lecka-Czernik, B. (2007) *Endocrinology* **148**, 2669–2680
- Watanabe, M., Houten, S. M., Mataka, C., Christoffolete, M. A., Kim, B. W., Sato, H., Messaddeq, N., Harney, J. W., Ezaki, O., Kodama, T., Schoonjans, K., Bianco, A. C., and Auwerx, J. (2006) *Nature* **439**, 484–489
- Yamauchi, T., Kamon, J., Waki, H., Terauchi, Y., Kubota, N., Hara, K., Mori, Y., Ide, T., Murakami, K., Tsuboyama-Kasaoka, N., Ezaki, O., Akanuma, Y., Gavrilova, O., Vinson, C., Reitman, M. L., Kagechika, H., Shudo, K., Yoda, M., Nakano, Y., Tobe, K., Nagai, R., Kimura, S., Tomita, M., Froguel, P., and Kadowaki, T. (2001) *Nat. Med.* **7**, 941–946
- Londos, C., Brasaemle, D. L., Schultz, C. J., Segrest, J. P., and Kimmel, A. R. (1999) *Semin. Cell Dev. Biol.* **10**, 51–58
- Puri, V., Konda, S., Ranjit, S., Aouadi, M., Chawla, A., Chouinard, M., Chakladar, A., and Czech, M. P. (2007) *J. Biol. Chem.* **282**, 34213–34218
- Fu, M., Rao, M., Bouras, T., Wang, C., Wu, K., Zhang, X., Li, Z., Yao, T. P., and Pestell, R. G. (2005) *J. Biol. Chem.* **280**, 16934–16941
- He, T. C., Sparks, A. B., Rago, C., Hermeking, H., Zawel, L., da Costa, L. T., Morin, P. J., Vogelstein, B., and Kinzler, K. W. (1998) *Science* **281**, 1509–1512
- Bezaira, V., Mairal, A., Ribet, C., Lefort, C., Girusse, A., Jocken, J., Laurencikiene, J., Anesia, R., Rodriguez, A. M., Ryden, M., Stenson, B. M., Dani, C., Ailhaud, G., Arner, P., and Langin, D. (2009) *J. Biol. Chem.* **284**, 18282–18291
- Kennell, J. A., and MacDougald, O. A. (2005) *J. Biol. Chem.* **280**, 24004–24010
- Bennett, C. N., Ross, S. E., Longo, K. A., Bajnok, L., Hemati, N., Johnson, K. W., Harrison, S. D., and MacDougald, O. A. (2002) *J. Biol. Chem.* **277**, 30998–31004
- Ross, S. E., Hemati, N., Longo, K. A., Bennett, C. N., Lucas, P. C., Erickson, R. L., and MacDougald, O. A. (2000) *Science* **289**, 950–953
- Modica, S., Murzilli, S., Salvatore, L., Schmidt, D. R., and Moschetta, A. (2008) *Cancer Res.* **68**, 9589–9594
- Lagathu, C., Christodoulides, C., Virtue, S., Cawthorn, W. P., Franzin, C., Kimber, W. A., Nora, E. D., Campbell, M., Medina-Gomez, G., Cheyette, B. N., Vidal-Puig, A. J., and Sethi, J. K. (2009) *Diabetes* **58**, 609–619
- Bhat, R. A., Stauffer, B., Komm, B. S., and Bodine, P. V. (2004) *Protein Expr. Purif.* **37**, 327–335
- Freytag, S. O., and Geddes, T. J. (1992) *Science* **256**, 379–382
- Fiorucci, S., Rizzo, G., Antonelli, E., Renga, B., Mencarelli, A., Riccardi, L., Morelli, A., Pruzanski, M., and Pellicciari, R. (2005) *J. Pharmacol. Exp. Ther.* **315**, 58–68